

Real-time Quantitative Analysis of L-Lysine Based on Radio Frequency Sensing

Kunal Wadhvani

CVEST

International Institute of Information
Technology (IIIT)

Hyderabad, India-500032

kunal.wadhvani@research.iiit.ac.in

Sheena Hussaini

MN Smart Radios, AD

Nokia of America Corporation

Dallas, TX, USA-75019

sheena.hussaini@nokia.com

Azeemuddin Syed

CVEST

International Institute of Information
Technology (IIIT)

Hyderabad, India-500032

syed@iiit.ac.in

Abstract—L-Lysine is an essential amino acid and bio-sample observing major significance in food processing, pharmaceutical and agricultural industries. Conventional sensing techniques require longer pre-processing times and are sensitive to ambient conditions. However, radio frequency (RF) sensing based on Complementary Split Ring Resonator (CSRR) exhibits a significant shift in the resonant frequency and is highly desirable for the L-Lysine's quantitative analysis. The frequency shifts of 498.4 MHz, 482.9 MHz, 471.4 MHz, 459.9 MHz and 452.3 MHz are obtained through varying concentrations from 0 mg/ml to 40 mg/ml in step size 10 mg/ml of L-Lysine solution. Therefore, experimental results and analysis presented in this work indicate the proposed radio frequency sensor's linearity in the above-reported concentration range.

Keywords—CSRR; L-Lysine; Radio Frequency Sensing; Quantitative Analysis

I. INTRODUCTION

Amino acids constitute the building blocks of proteins classifying into essential and non-essential amino acids. Essential amino acids are not synthesized by the human body hence supplemented through diet. L-Lysine is an essential amino acid, plays a vital role and participates in important life processes. For example, L-Lysine forms collagen in the presence of proline and vitamin C [1]. It is a precursor of L-carnitine, involved in mitochondria oxidation necessary for the cell development process [2]. L-Lysine deficiency is prevalent among individuals with plant-based diet affected using nitrogenous fertilizers compared to those with animal protein diet [3, 4]. Hence, used as a vital marker for the nutritional value of food products and crops. In short-term, dietary supplements derived from food products and drugs helps in increasing the lysine levels. Still, both agriculture and food processing industries need an effective long-term solution for monitoring the L-Lysine levels. Additionally, L-Lysine also plays a vital role in the pharmaceutical sector exploited for its antibacterial and antiviral actions against E. coli and herpes simplex virus [5]. Thus, quantitative analysis of lysine is of utmost significance in today's food processing, pharmaceutical and agricultural industries.

The latest analytical methods for quantitative analysis of L-Lysine, such as chromatography [6], enzyme-based amperometric bio-sensing [3, 7] and colorimetry [8] require expensive reagents, longer processing time and skilled technicians for instrument control. Moreover, enzyme-based

sensors suffer from instability due to their intrinsic nature constraining the need for environment control, whereas colorimetric sensors suffer from non-reusability. Therefore, a less cumbersome, robust and reusable technique is needed.

Radio frequency (RF) sensors for material characterization based on dielectric constant properties have gained much attention recently due to their biomedical, food processing and electronics engineering applications for their minimally invasive, cost-effective and label-free nature [9]. Microwave sensors are classified broadly into resonant and non-resonant. Non-resonant sensors used for broadband characterization provide moderate accuracy and slower response time. In contrast, resonant sensors offer better precision over a narrow band of frequencies [10], high sensitivity, cost-effectiveness and faster response time desirable for real-time analysis. Amongst resonant sensors, planar resonant sensors such as complementary split ring resonators (CSRR) [11, 12], and splitting resonators (SRR) [13] are preferable for quantitative analysis of bioliquids due to simple geometry, compactness and fabrication ease.

In this paper, the RF sensor of size 38 x 32 mm² is designed with resonant frequency at 1.51 GHz, fabricated on a 1.6 mm thick FR4 substrate with copper of thickness 0.035 mm on both sides. The fabricated sensor was connected to the Keysight Vector Network Analyzer (VNA), and a sample was dropped on the high sensitivity region of the sensor. Varying concentrations of L-Lysine solution are prepared using Phosphate buffer as the solvent. The transmission coefficient (S_{21}) has been analyzed in this work where the shift in the resonant frequency property used for distinguishing between varying concentrations of solutions.

II. SENSOR DESIGN AND SIMULATION

The proposed sensor comprises a microstrip line coupled to CSRR, as shown in Fig. 1 where the yellow portion represents

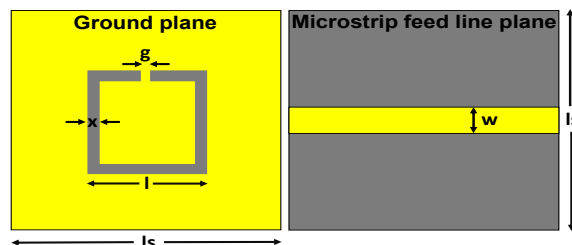


Fig. 1. Front and back view of designed sensor

the conductor over the substrate and the grey portion represents the substrate where the conductor is etched out. On one side of the sensor, we have a microstrip line from where the electromagnetic wave is fed, known as the feed line. On the other side is a ground plane from which the CSRR is etched out. In Fig. 1, 'g' is the width of the small conductor connecting the center square copper plate and the ground plane, 'x' is the width of the etched portion of CSRR, 'l' is the length of CSRR, 'ls' is the length of the microstrip line and 'w' is the width of the microstrip line.

Fig. 2(a) shows the equivalent lumped circuit diagram of the sensor for the resonant frequency at 1.51 GHz, where R, L and

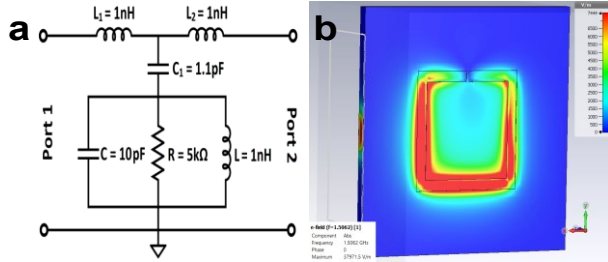


Fig. 2. (a) Equivalent lumped circuit for sensor (b) Electric field distribution across the CSRR.

C models the CSRR. R represents the loss due to the CSRR, L represents the inductance due to the small conductor of width 'g' and C represents the capacitance between the center square copper plate and the ground plane. L1, L2 and C1 represent the inductances and capacitance of microstrip feed line, respectively [11].

The dominant phenomenon in the excitation of CSRR by the electromagnetic wave caused due to electrical coupling makes it a suitable candidate for material detection, exhibiting a change in permittivity. The high sensitivity region of the sensor has been analyzed based on the field distribution. In Fig. 2(b) shows that the electric field is maximum at the lower and side edges of the capacitive cavity serving as a suitable position for placing the dielectric samples. As the sample is placed in the detected high sensitivity region, change in permittivity occurs, which in turn changes the capacitance of the CSRR. The capacitance change leads to a change in the sensor's resonant frequency, indicating the detection of the sample. The resonance condition is observed when the electrical energy in the capacitors C and C1 is equal to the magnetic energy stored in the inductor L. In accordance with

the lumped model, the resonant frequency of the CSRR is given by (1) as reported in [14]:

$$f_r = \frac{1}{2\pi\sqrt{L(C_1 + C)}} \quad (1)$$

III. EXPERIMENTAL RESULTS AND DISCUSSION

The designed sensor is fabricated on a 1.6 mm thick FR4 substrate with copper of thickness 0.035 mm on both sides, as shown in Fig. 3(a). Green mask of the epoxy resin material is deposited over the copper, which has thickness the same as

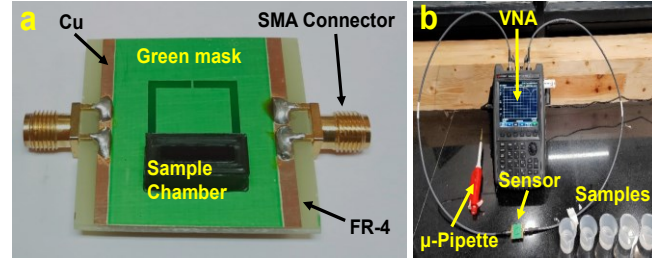


Fig. 3. (a) Fabricated sensor (b) Experimental setup

copper. The mask is biocompatible and is used to prevent any reaction of copper with samples dropped over the sensor. A sample chamber of PLA material is 3D printed to form a wall around the sensor's high sensitivity region. This is done to confine the liquid sample to be dropped within the chamber and eliminate the human error in dropping the sample. The gap within the sample chamber is 2.5 mm.

SMA connectors are soldered on the copper region of the sensor to connect to the VNA. The sensor is then connected to the VNA to record the transmission coefficient (S_{21}), as shown in Fig. 3(b). Phosphate buffer (PB) of concentration 0.1M is prepared by dissolving 3.4 gm of PB in 1 litre of deionized (DI) water. Phosphate buffer solution (pH=7.2) is used as a standard solution for dissolving L-Lysine to maintain a constant pH of the final solution. Then four different concentrations of L-Lysine solution varying from 10 mg/ml to 40 mg/ml have been prepared by performing dilution of L-Lysine in PB solution by constant stirring. Using a micropipette, a fixed volume of 50 μ l is dropped in the sample chamber placed above the sensor's sensitive region, where the electric field is maximum. The experimental procedure is repeated multiple times for verifying the result

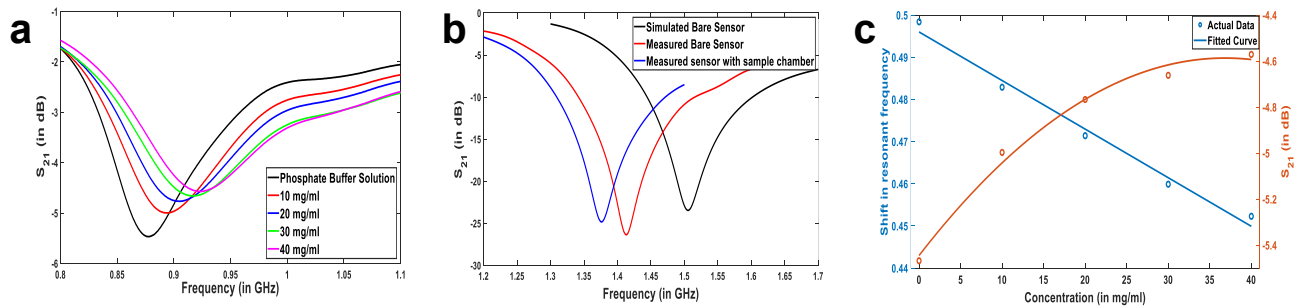


Fig. 4. (a) Magnitude of S_{21} versus resonant frequency variation for concentration of L-Lysine solutions from 0 – 40 mg/ml. (b) Magnitude of S_{21} versus resonant frequency for simulated bare sensor, measured bare sensor and measured sensor with sample chamber. (c) Variation of shift in resonant frequency and magnitude of S_{21} with change in concentration of L-Lysine solution.

accuracy and measurement repeatability. The experiments were conducted at room temperature and normal ambient conditions.

The resonant frequency of the empty sensor is obtained at 1.41 GHz, whereas the resonant frequency of the empty sensor with a sample chamber is obtained at 1.376 GHz, as shown in Fig. 4(b). Therefore, we take 1.376 GHz as the reference for calculating the sensor's resonant frequency shift when various concentrations of L-Lysine solution are placed over the sensor. The shift in resonant frequency is given by:

$$\Delta f = f_r - f \quad (2)$$

Where, f_r and f are resonant frequency of sensor with sample chamber and varying concentrations of L-Lysine solution placed on it. Due to the limitations in the fabrication process, environmental effects around the experimental setup and uncertainty in the substrate's dielectric constant, the simulated and experimental resonant frequencies of the sensor do not match exactly as seen in Fig. 4(b).

The shift in the resonant frequency for PB aqueous solution (0 mg/ml) is measured as 498.4 MHz with a measured standard deviation of 3.5 MHz, frequency shifts of 482.9 MHz, 471.4 MHz, 459.9 MHz and 452.3 MHz with a measured standard deviation of 3.0 MHz, 2.7 MHz, 1.7 MHz and 2.0 MHz are obtained for concentrations of 10 mg/ml, 20 mg/ml, 30 mg/ml and 40 mg/ml respectively. These shifts indicate the designed sensor's sensitivity in distinguishing the concentration change of the L-Lysine solution. The magnitude of S_{21} for PB aqueous solution is obtained at -5.468 dB. Similarly, the magnitude of S_{21} for concentrations 10 mg/ml, 20 mg/ml, 30 mg/ml and 40 mg/ml are obtained at -4.997 dB, -4.767 dB, -4.662 dB and -4.571 dB respectively. We have applied the curve fitting tool of MATLAB to the experimental data obtained above and developed the following equations (3) and (4) given below. The actual data and fitted curves are shown in Fig. 4(c).

$$\Delta f = -0.001152 \times C + 0.496 \quad (3)$$

$$S_{21} = -0.0006321 \times C^2 + 0.04658 \times C - 5.445 \quad (4)$$

$$(R^2=0.9861 \text{ for eqn. (3) and } R^2=0.99 \text{ for eqn. (4)})$$

where Δf is shift in resonant frequency, C is concentration of L-Lysine solution and S_{21} is magnitude of transmission coefficient.

The change in the resonant frequency and S_{21} are observed due to the electromagnetic interaction of the sensor and L-Lysine solutions. It has been observed that as the concentration of L-Lysine is increased, the dielectric constant of the solution is reduced, increasing the resonant frequency and hence, the shift in the resonant frequency decreases as shown in Fig. 4(a). Also, as the concentration of L-Lysine is increased, the magnitude of S_{21} increases non-linearly given by equation (4). Hence, any of the above two parameters can be used as an indicator for varying concentrations of L-Lysine. In Fig. 4(c), we observe that the shift in resonant frequency and magnitude of S_{21} follows a linear relationship with the concentration given by equation (3), indicating the linear behavior of the proposed sensor. As reported in [15] for the L-Lysine aqueous solution,

it can also be verified that the dielectric constant decreases with an increase in the concentration of the solution.

IV. CONCLUSION

In this paper, we proposed RF sensing as an alternative method for the quantitative analysis of L-Lysine. The demonstrated results in our work indicate the linearity of the sensor suitable for effective detection of the concentration variation of L-Lysine. Therefore, the proposed method of RF sensing is not ambient specific, simple, easy to perform, robust, reusable and linear. In the future, the RF sensing technique can also be extended for the quantitative analysis of other essential amino acids.

REFERENCES

- [1] T. Y. Hendrawati, R. A. Nugrahani, A. I. Ramadhan, S. Susanty and A. Siswahyu, "The Effects of Vacuum Evaporation on Amino Acid Contents in Pureed Aloe Chinensis Baker Gel using HPLC," *IOP Conf. Ser.: Mater. Sci. Eng.*, vol. 543, p. 012014, 2019.
- [2] Tome Daniel and Bos Cecile, "Lysine Requirement through the Human Life Cycle," *The Journal of Nutrition*, vol. 137, no. 6, Jan. 2007.
- [3] E. Akyilmaz, A. Erdogan, R. Ozturk and I. Yasa, "Sensitive determination of L-Lysine with a new amperometric microbial biosensor based on *Saccharomyces cerevisiae* yeast cells," *Biosens. Bioelectron.*, vol. 22, no. 6, pp. 1055–1060, 2007.
- [4] A. Shahverdi *et al.*, "Concentration changes of Lysine and Methionine amino acids in potatoes varieties affected by different levels of Nitrogen fertilizer," *Tech. J. Eng. Appl. Sci.*, vol. 2, no. 4, pp. 93–96, 2012.
- [5] D. Datta, A. Bhinge and V. Chandran, "Lysine: is it worth more?," *Cytotechnology*, vol. 36, no. 1–3, pp. 3–32, 2001.
- [6] A. Hernandez, M. A. Serrano, M. M. Munoz and G. Castillo, "Liquid Chromatographic Determination of the Total Available Free and Intrachain Lysine in Various Foods," *J. Chromatogr. Sci.*, vol. 39, no. 1, pp. 39–43, 2001.
- [7] R.-I. S.-V. Staden, R. A. M. Nejem, J. F. V. Staden and H. Y. Aboul-Enein, "Amperometric biosensor based on diamond paste for the enantioanalysis of L-Lysine," *Biosens. Bioelectron.*, vol. 35, no. 1, pp. 439–442, 2012.
- [8] Y. Zhou, Z. Yang and M. Xu, "Colorimetric detection of lysine using gold nanoparticles aggregation," *Anal. Methods*, vol. 4, no. 9, pp. 2711, 2012.
- [9] G. Vlachogiannakis *et al.*, "A Compact Energy Efficient CMOS Permittivity Sensor Based on Multiharmonic Downconversion and Tunable Impedance Bridge," *IEEE International Microwave Biomedical Conference (IMBioC)*, pp. 1–3, 2018.
- [10] P. Porwal, A. Syed, P. Bhimalapuram, T. K. Sau, "Design of fractal geometry based RF sensor for detection of complex permittivity of unknown sample," *Proc. IEEE Asia Pac. Microw. Conf.*, pp. 1310, 2017.
- [11] A. Ebrahimi, W. Withayachumnankul, S. Al-Sarawi, D. Abbott, "High-sensitivity metamaterial-inspired sensor for microfluidic dielectric characterization," *IEEE Sensors J.*, vol. 14, no. 5, pp. 1345–1351, 2014.
- [12] D. Mondal, N. K. Tiwari and M. J. Akhtar, "Microwave Assisted Non-Invasive Microfluidic Biosensor for Monitoring Glucose Concentration," *IEEE Sensors*, pp. 1–4, 2018.
- [13] R. Narang *et al.*, "Sensitive, Real-time and Non-Intrusive Detection of Concentration and Growth of Pathogenic Bacteria using Microfluidic-Microwave Ring Resonator Biosensor," *Sci. Rep.*, vol. 8, no. 1, 2018.
- [14] J. Bonache, M. Gil, I. Gil, J. Garcia-Garcia and F. Martin, "On the electrical characteristics of complementary metamaterial resonators," *IEEE Microwave and Wireless Components Letters*, vol. 16, no. 10, pp. 543–545, Oct. 2006.
- [15] X. Liao, G. Raghavan, G. Wu and V. Yaylayan, "Dielectric properties of lysine aqueous solutions at 2450 MHz," *J. Mol. Liq.*, vol. 107, no. 1–3, pp. 15–19, 2003.